The influence of material aging on the structural behavior of a flexible roof with a polymer membrane shell

Andrei V. Chesnokov* iD, Vitalii V. Mikhailov iD, Ivan V. Dolmatov iD

The Faculty of Civil Engineering, Lipetsk State Technical University, Moskovskaya street 30, 398600 Lipetsk, Russian Federation.

Abstract

The roof structure considered in the research consists of continuous cables and a number of spreaders forming a three-dimensional frame. The frame is covered with a polymer membrane made of flexible architectural fabrics. The elements of the roof are compact and suitable for transportation to remote construction sites. The roof also has advantages for developing areas with harsh climatic conditions.

The flexible elements of the roof, however, only provide transmission of tensile forces. Under compression, cables slacken and the membrane becomes wrinkled. Pre-tension of the flexible elements, which is introduced to retain the operability of the roof, tends to gradually diminish due to material aging. The aging results in the alteration of strength properties and creep elongation of the structural elements. It induces membrane tearing on local areas.

Force alteration in primary structural members is examined in the present study, with statistical methods used for data analysis. They include significance hypothesis testing and correlation coefficients estimation. The data are obtained by the Finite Element simulation of the roof using EASY-2020 software.

The results of the work may be used for life expectancy assessment of flexible roof structures, providing important information for the preliminary design stage. The work contributes to the safety enhancement of cable-membrane structures and the expansion of their scope in permanent building constructions.

Keywords: polymer membrane aging, creep, stress relaxation, pre-stressed cable roof

1. Introduction

The roof structure considered in the research consists of pre-stressed flexible cables and a number of spreaders, forming a three-dimensional frame. The frame is covered with a polymer membrane made of architectural fabrics (Fig. 1) (Chesnokov & Mikhailov, 2017a, 2017b).
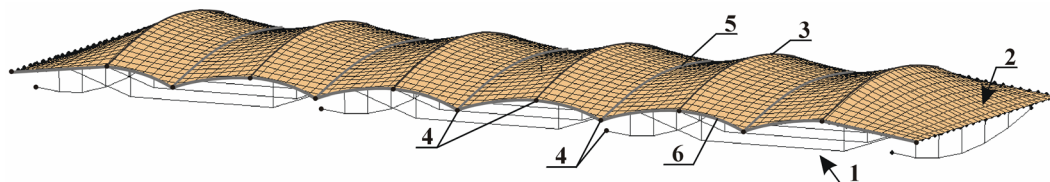
Fig. 1. The roof structure: 1 – three-dimensional frame, 2 – polymer membrane shell, 3 – rib, 4 – fixed support, 5 – backstay cable, 6 – catenary cable

The membrane is laid on vertical ridges of the frame and pre-tensioned by backstay and catenary cables. Pre-tensioning is needed to avoid wrinkles in the membrane and to keep the operability of the overall roof construction.

The frame of the roof may be represented as a number of successively arranged sections which equilibrate each other (Fig. 2).

Bearer cables are situated in mutually perpendicular directions. Longitudinal bearer cables are fixedly attached to columns of the building, while transverse cables are supported with spreaders which are installed on the longitudinal cables.

Vertical ribs are formed by ridge cables and spreaders which are supported by transverse cables. Ridge cables and ties compose the top chord of the frame.

The roof considered in the research is a low-weight translucent structure. It is architecturally impressive, allowing large distances between columns of the building. The overall height of the roof is lower in comparison to ordinary membrane structures of the same span (Chesnokov et al., 2018). The elements of the roof are compact and suitable for transportation to remote construction sites. The roof also has advantages in developing areas with harsh climatic conditions.

On the other hand, the flexible elements of the roof only provide transmission of tensile forces. Under compression, the cables and the membrane slacken, causing potential instability of the construction. Pre-stressing of the roof tends to gradually diminish due to material aging. Aging results in the alteration of strength properties, as well as in stress relaxation and creep.

Aging also induces membrane tearing in local areas. The tearing tends to occur in overstressed zones, brought about by external impacts which were not properly considered in the design stage. Rigid edges of bearing structures and point supports form peak stressed areas (Monjo-Carrio, 2015; Fiúza, 2016).

Tearing, however, may be a result of complex processes on a material level. A slit can emerge in loaded and unloaded zones of the membrane, becoming accidental. The emergence of a multitude of tiny defects hardly results in structural collapse. On the other hand, their influence on the roof's behavior under load and on the operational reliability of the construction should be investigated.

Simulating the process of polymer membrane aging has been performed by Suleymanov (2006), with the destruction sequence and influence of operational factors studied. Experimental investigations pointed out the areas of membrane specimens which are more susceptible to microstructural defects and tend to fail under external impacts. The multivariate mathematical model developed by Suleymanov (2006), includes interactions between membrane yarns and the coating. It takes into account the visco-elastic properties of the materials.

Technical defects (Wang et al., 2015) caused by material aging reduce the durability of flexible cables and polymer membrane more intensively than for ordinary materials which have a homogeneous structure. A methodology for estimating polymer composite longevity has been proposed by Mukhamedova (2005). The technique takes into account micro-level destruction of the material and the influence of UV radiation.

The durability of the polymer membrane when subjected to adverse external impacts has been investigated by Kupriyanov (1986) experimentally, and techniques for accelerated laboratory estimates of the membrane aging process are proposed. This study allows the forecasting of the longevity of new materials given the expected operational conditions.

The long-term behavior of polymer membranes was investigated by Asadi et al. (2017). Strength reduction factors were assessed for glass-PTFE and polyester-PVC membranes. Environmental impacts on the yarns and the process of top coat weathering were studied.
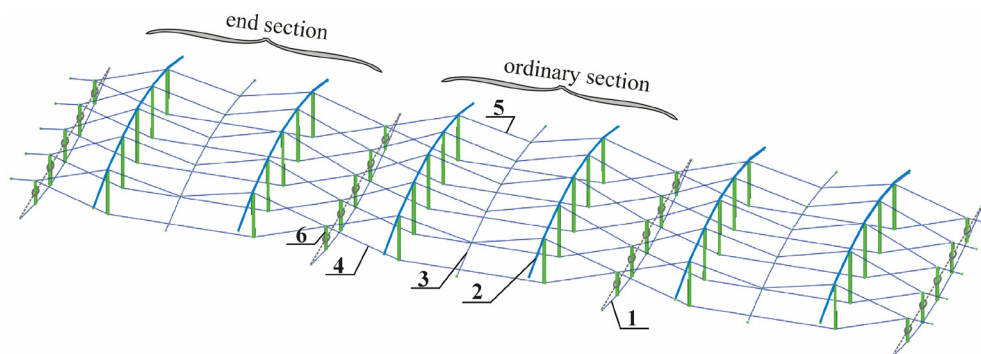
Fig. 2. The frame of the roof: 1 – longitudinal bearer cable, 2 – ridge cable, 3 – longitudinal tie, 4 – transverse bearer cable, 5 – transverse tie, 6 – spreader

Polymer membrane and steel cables are also susceptible to creep, where creep is a rheological property of a material. It can be mitigated by pre-stretching the material before embedding in the construction and by means of pre-tensioning the whole construction during its installation on site.

The creep behavior of polymer membrane has been investigated by Mukhamedova (2005). Mathematical models for simulating composites were developed and material constants were given in this dissertation. They allow for the inelastic deformation of a membrane with time to be calculated.

Creep, however, cannot be avoided completely. It causes rainwater ponding and 'flapping' of the membrane under the wind load, resulting in fatigue damage (Bridgens et al., 2004).

The influence of material creep on the structural behavior of flexible roofs needs to be clarified, with the long-term creep behavior of polymer membrane and steel cables requiring further study. The need to re-tension the membrane during the operational stage, its periodicity and required stress level of adjustment are to be investigated.

The probabilistic nature of the aging process and the complexity of flexible roof's structural behavior require statistical methods to be employed. Statistical methods are successfully used for predicting the safety index of membrane structures, considering uncertainty in external loads and material properties (Gosling et al., 2012).

2. Method

2.1. General considerations

Membrane damages and creep elongation of the structural elements are considered in the present study for simulating the material aging phenomenon. It is assumed that the membrane gets damaged in the form of local slits. Slit locations, taken into account, are shown in Figure 3.

Creep elongation ε_c of the roof's element is introduced into the structural model by means of variation of its unstressed length. The elongation is taken from the range:

$$\varepsilon_c \in [0.0, ..., \varepsilon_p], \qquad (1)$$

where ε_p is a long-term relative elongation (Fig. 4), which is specific for the given material.

Statistical methods are used for estimating the influence of material aging on axial forces N in the steel cables. The forces are obtained through the analysis of the roof using commercial software for non-linear structural simulation EASY-2020 (Technet GmbH, 2019).
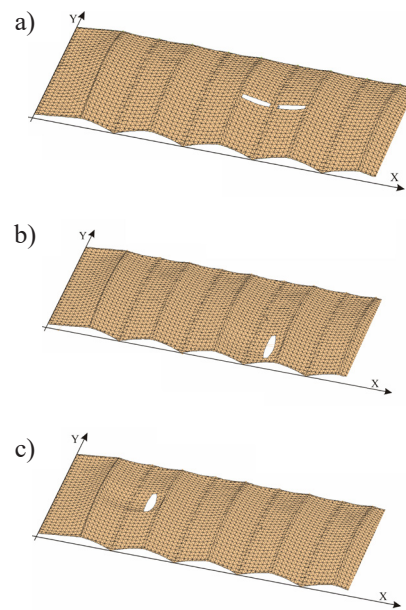
Fig. 3. Membrane damages, considered in the research: a) slits in the ordinary section of the roof along the X-axis; b), c) slits along the Y-axis in the ordinary and end sections, respectively
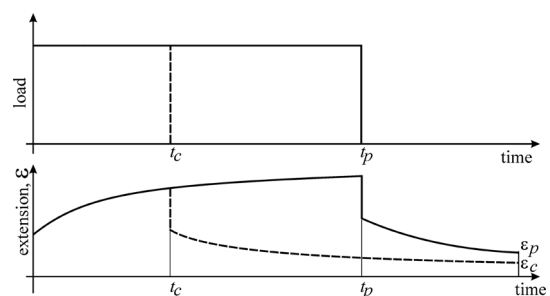

Fig. 4. Typical creep curves

The following stages are involved in the process of the static analysis:
- finding the membrane shape by the Force Density Method;
- holistic Finite Element Analysis of the membrane and the frame of the roof.

In the first stage, the membrane is substituted by a mesh. Unknown nodal coordinates of the mesh are obtained from a set of linear equations given initial stresses (pre-stressing), boundary conditions, and approximate mesh size along the X and Y axes (Ströbel et al., 2016; Tibert, 1999).

Coupling the membrane and the bearer frame results in the finite element model of the roof (Fig. 5). The model consists of pin-joint straight elements. Structural members of the roof are able to sustain axial forces only, thus, each node of the model has three degrees of freedom.
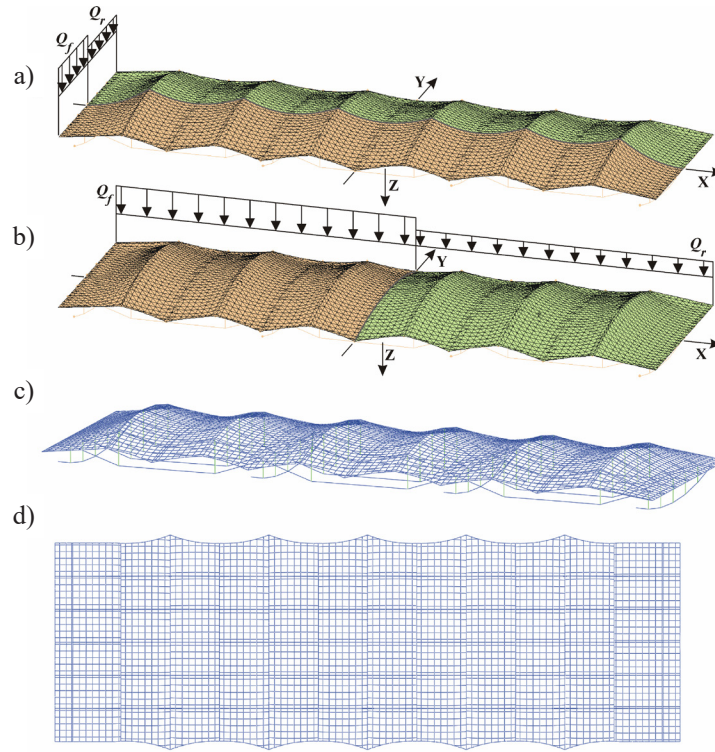
Fig. 5. External loads, influencing the roof (a, b) and the finite element model (axonometric and the top view) (c, d)

Finite Element Analysis of the roof is performed using the BEAM-module of the EASY system. The analysis is implemented in an iterative way by minimizing unbalanced forces in each node of the construction. Thus, geometrically non-linear behavior of roof is considered.

External loads Q, influencing the roof, are applied on triangular elements, forming the membrane (Figs. 5a and 5b). The triangular elements are automatically generated by the EASY system in order to redistribute external impacts throughout the nodes of the structural model. They are not directly used for finite element simulation.

The loads consist of two parts (Fig. 5): the full load Q_f and the reduced load Q_r. A reduction factor $k_r \in [0...1]$ simulates nonuniform impacts on the construction:

$$Q_r = k_r \cdot Q_f. \tag{2}$$

Membrane slits are simulated by means of dropping out of particular finite elements (links) which constitute the polymer membrane in the structural model. Because membrane damage can only take two levels (the slit is either present or not), its influence on the roof structure is investigated by means of significance hypothesis testing. On the other hand, the creep elongation takes several intermediate levels in the range (1). Thus, the creep impact is estimated using the correlation between considered element elongations ε_c and the force in the corresponding element.

2.2. Testing the hypothesis of significance

The following null hypothesis H_0 is tested: "axial force N in the element of the roof is not affected by material aging". The Student's test is used to examine H_0:

$$|T| > q_{\frac{\alpha}{2}} \tag{3}$$

where $q_{\alpha/2}$ is the $(1 - \alpha/2)$ – quantile of the Student's distribution, and T is the test statistic (Rice, 2007):

$$T = \frac{\overline{X}_{n_x} - \overline{Y}_{n_y} - \Delta\mu}{\sqrt{\dfrac{\tilde{S}_X}{n_x} + \dfrac{\tilde{S}_Y}{n_y}}} \tag{4}$$

where $\overline{X}_{n_x} = \sum_{i=1}^{n_x} N_i^\xi / n_x$ and $\overline{Y}_{n_y} = \sum_{i=1}^{n_y} N_i^0 / n_y$ are the sample means of the force values in element i of the roof, the upper index '0' denotes the reference state of the construction (no material aging is present), while the index ξ is applied for taking into account aging of particular structural elements (deteriorated state), n is the number of values considered, $\tilde{S}_X = 1/(n_x - 1) \cdot \sum_{i=1}^{n_x} (N_i^\xi - \overline{X}_{n_x})^2$ and $\tilde{S}_Y = 1/(n_y - 1) \cdot \sum_{i=1}^{n_y} (N_i^0 - \overline{Y}_{n_y})^2$ are the sample variances, $\Delta\mu$ is the difference between the expected

means of the forces, obtained for deteriorated and the reference states of the roof:

$$\Delta\mu = \mu_{N^\xi} - \mu_{N^0} \qquad (5)$$

Under the null hypothesis, the expected means are considered equal for both the reference state and the construction with deteriorated elements due to aging. Thus, $\Delta\mu = 0$.

The probability p is obtained from the Student's $t_{p,v}$ – distribution table (Rice, 2007), given the test statistic value T (4) and the number of degrees of freedom $v = \min(n_x, n_y) - 1$:

$$|T| = t_{p,v} \qquad (6)$$

The confidence level α and the corresponding reliability of rejecting the null hypothesis are obtained as follows:

$$\alpha = 2 \cdot (1 - p) \qquad (7)$$
$$\gamma = 1 - \alpha \qquad (8)$$

The higher the γ-value, the more confidently the null hypothesis H_0 can be rejected, meaning that the considered aging phenomenon significantly affects on the axial force in the structural element.

Examining the null hypothesis H_0 gives a qualitative estimation of an axial force's dependence on the particular aging phenomenon in the membrane. Quantitative estimation of the dependence is obtained by the ratio:

$$\delta = \frac{N^\xi - N^0}{N^0} \cdot 100\% \qquad (9)$$

where δ is a variation of axial force in a structural element given particular external loads.

2.3. Estimating the material creep influence on the structural behavior of the roof

Creep is a permanent elongation of the material, which is subjected to external loads. The unstressed length of a structural element, subjected to creep, is obtained as follows:

$$l_{0,c} = l_0 \cdot (1 + \varepsilon_c) \qquad (10)$$

where: l_0 is the initial element's length, while ε_c is the element's elongation (1), which corresponds to a particular creep level.

The initial length l_0 includes pre-tensioning Δl_{pr} of the element, implemented for providing initial stresses in the construction:

$$l_0 = l_g^0 - \Delta l_{pr} \qquad (11)$$

where l_g^0 is a geometrical element length, which is equal to the distance between element's nodes in an undeformed state.

Correlation coefficient ($\rho_{X,Y} \in [-1.0 \ldots +1.0]$) between axial forces and creep elongations of structural elements is obtained as follows:

$$\rho_{X,Y} = \frac{\text{cov}(X,Y)}{\sqrt{\text{var}(X) \cdot \text{var}(Y)}} \qquad (12)$$

where: X is a set of axial forces values; Y is a set of the corresponding creep elongations ε_c (1) of particular structural elements; $\text{var}(X)$, $\text{var}(Y)$ and $\text{cov}(X, Y)$ are variances and covariance of X and Y datasets.

The closer the absolute value $|\rho_{X,Y}|$ to 1.0, the stronger the correlation between the creep elongation and the forces in the considered element.

3. Results and discussion

3.1. The roof structure

A roof consisting of three sections is considered (Figs. 1 and 2). The geometrical dimensions of a section are shown in Figure 6.

The top and bottom chords of the roof's frame are made of high strength stainless steel cables (open spiral strands) with the modulus of elasticity E_{cab} = 130 GPa (ETA-11/0160, 2018). Long-term creep elongation of the cables is taken the following: ε_p = 0.05%. Diameters of transverse and longitudinal bearer cables are 24 mm and 32 mm, respectively. For the ridge cables and the ties, diameters 14 mm and 6 mm are adopted. Backstay and catenary cables are 10 mm in diameter.
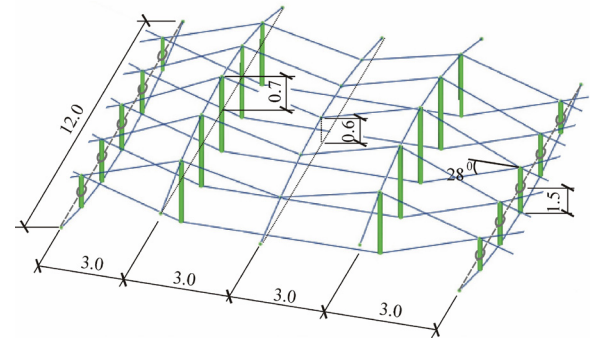

Fig. 6. A section of the roof, considered as an example (dimensions are indicated in meters)

The membrane shell of the roof is made of architectural fabric. It comprises a polyester net, PVC coating, and PVDF surface treatment. Considering the fabric "Flexlight Advanced 1502 S2", which is produced by the Serge Ferrari Group (2021), the breaking strength values of the membrane are the following: σ_u = 200 kN/m – in the warp direction (along the X-axis) and σ_u = 160 kN/m – in the weft direction (along the Y-axis). The creep elongations ε_p are adopted 0.6 and 1.25%, while the membrane stiffnesses are taken 1200 kN/m and 800 kN/m in the warp and weft directions, respectively.

The full load Q_f, influencing half of the roof (Figs. 5a and 5b), is taken from the set [0.36, 0.72, 1.08, 1.44, 1.8] kPa, while the reduction factor k_r takes six values from [0.0, 0.2, 0.4, 0.6, 0.8, 1.0] .

3.2. Adoption of the slit length and simulation of tear propagation

Besides axial force variation in the elements of the structural frame, membrane damages also induce stress redistribution in the shell of the roof. It results in wrinkle formation and the emergence of overstressed zones (Fig. 7).

Slit lengths are adopted under the ultimate limit state condition, applied for the membrane:

$$\sigma_m \leq \sigma_y \qquad (13)$$

where: σ_m is the membrane peak stress, brought about by the slit; σ_y is the membrane limit tension.

The limit tension σ_y is equal to the membrane breaking strength σ_u, divided by the safety factor K = 5.0 (Forster & Mollaert, 2004):

$$\sigma_y = \frac{\sigma_u}{K} \qquad (14)$$

For the "Flexlight Advanced 1502 S2" fabric, the limit tensions σ_y are 40 kN/m and 32 kN/m in the warp and weft directions, respectively.

Considering the mesh density $l_{wr} \times l_{wf}$ = 0.4 m × 0.4 m and starting from a slit of 1.2 m long (Fig. 7a), the resultant slit length is obtained in a step-by-step manner under the condition (13): $L_{slit,\lim}$ = 2.8 m (Fig. 8g).

Having exceeded the ultimate limit state condition (13), membrane stresses will induce tear propagation throughout the surface. In the Y-direction, the tearing is only confined by catenary cables, which are situated on the opposite sides of the roof. Thus, the tearing is likely to propagate throughout the whole span (Fig. 7b). Along the X-axis, the tearing tends to self-extinguish due to the comparatively small distance between the ridge and the backstay cables (Fig. 7c).
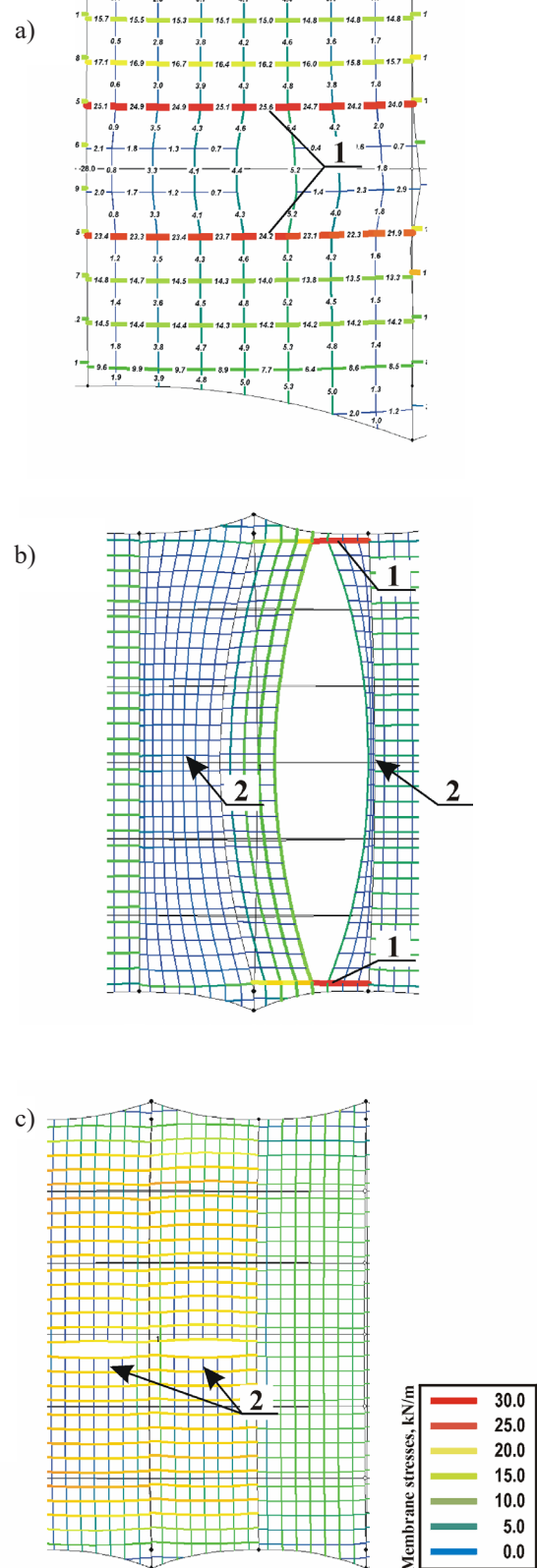
Fig. 7. The shell with damages (membrane stresses are indicated in [kN/m]): a) initial slit 1.2 m long in the Y direction; b) propagation of the slit throughout the whole surface; c) the slits along the X-axis, 1 – peak stresses, 2 – wrinkles (slackened zones)
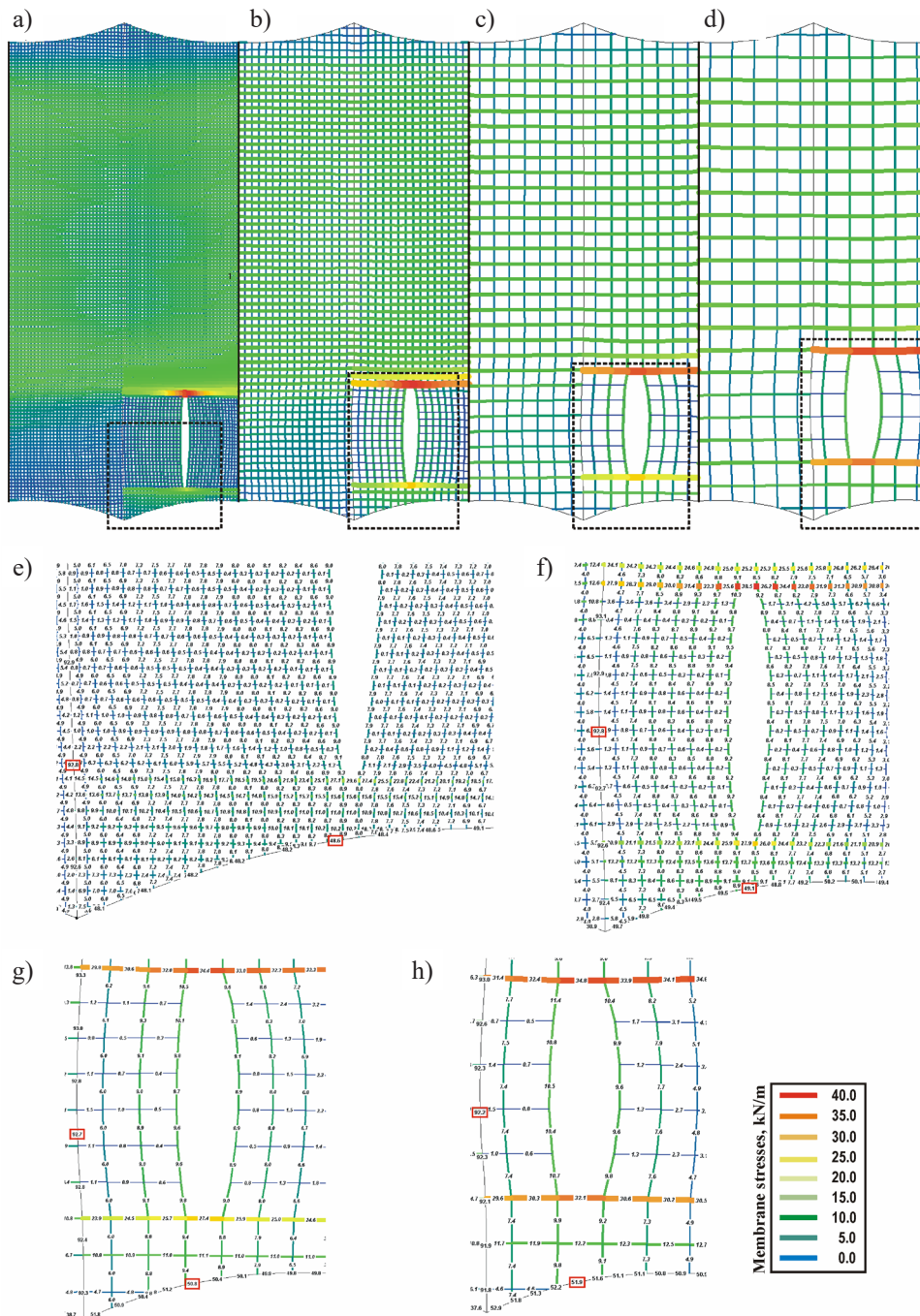
Fig. 8. General charts of membrane stresses in the shell [kN/m] and axial forces in the cables [kN] given the length of the slit $L_{slit} = 2.8$ m, and the mesh sizes: a) $l_w = 0.1$ m; b) $l_w = 0.2$ m; c) $l_w = 0.4$ m; d) $l_w = 0.6$ m; e), f), g), h) enlarged views of fragments, marked by a dashed line

3.3. Mesh sensitivity study

For membrane discretization, the regular mesh type is adopted. Finite elements forming the mesh are arranged in two perpendicular directions (along X and Y axes). Thus, the mesh is composed of a multitude of internal rectangular cells with size $l_{wr} \times l_{wf}$ in the warp and weft direction, respectively, and complex-shaped cells at the boundaries. Considering squared internal cells, $l_{wr} = l_{wf} = l_w$, different mesh sizes l_w are examined in order to study the mesh

density influence on the stress state of the membrane, as well as catenary and backstay cables (Fig. 8).

Particular sections in the figure, marked by letters a–d, are independent. They are separated by the ribs (Fig. 1, element 3), which are held stationary for the mesh sensitivity study. Enlarged views of a fragment of each section, marked by a dashed line, are shown under letters e–h. Stresses in the mesh, as well as axial forces in the backstay and catenary cables, are indicated in Figure 8. The forces are highlighted with red rectangles.

Figure 8 shows that axial forces in the backstay and catenary cables exhibit small variation with the mesh size. This variation will insignificantly influence the results of the present work. Finer mesh provides a smoother distribution of stresses in the membrane than a coarser one does. On the other hand, finer meshes require a lot of resources to be analyzed. In order to keep a balance between stress distribution smoothness and computational cost, the mesh size $l_w = 0.4$ m is adopted for the present study.

3.4. Estimating the influence of material aging on roof's behavior

The cables of the roof are split into six types, denoted by the first digit in the element number (Figs. 9a and 9b). The null hypothesis H_0 is examined for principal elements of the roof. Reliabilities γ (8), calculated for three membrane damage scenarios (Fig. 3), are in Table 1.

The table shows the significant influence of membrane damage on forces in backstay and catenary cables (elements of types 5 and 6). The graphs of δ-ratios (9) for all load cases (Fig. 10) indicate that membrane tearing causes growth of axial forces in the backstay cables 5 up to 65%. Catenary cables 6 are also overstressed by up to 60% if the slit in the membrane is along the Y-axis. Membrane tearing along the X-axis results in slackening of the catenary cables up to 50%.

Longitudinal ties 3 are susceptible to membrane tearing along the Y-axis (Figs. 3b and 3c). The behavior of the ties is similar to the backstay cables' behavior, but the force increasing is confined by 30%.

With regard to the longitudinal bearer cables 1, the adopted null hypothesis cannot be rejected, meaning a very negligible effect brought about by membrane aging. Transverse bearer cables 4 and ridge cables 2 are significantly affected by membrane tearing along the

Y-axis in the middle of the roof's span (Fig. 3c). The forces in the bearer cables tend to diminish with membrane tearing, while the ridge cables are overstressed. For both types of cables, the absolute force variation is confined by 30%.

Table 1. Reliabilities γ for rejecting the null hypothesis H_0

Designation of cable	Membrane damage		
	Figure 3a	Figure 3b	Figure 3c
ridge cables			
2.1	–	–	**0.910**
2.2	–	–	0.691
2.3	–	0.804	0.839
longitudinal ties			
3.1	–	0.855	**0.963**
3.2	0.761	**0.969**	–
transverse bearer cables			
4.1	–	0.659	–
4.2	–	0.538	**0.953**
4.3	–	0.608	0.634
4.4	–	–	0.836
backstay cables			
5.1	–	–	0.817
5.2	**0.995**	**0.979**	–
catenary cables			
6.1	–	–	**0.991**
6.2	–	–	**0.997**
6.3	**0.925**	**0.961**	–
6.4	**0.993**	**0.998**	–

Reliabilities less than 0.5 are skipped and reliabilities greater than 0.9 are highlighted in bold

Correlation coefficients (12) between axial forces and creep elongations of structural elements are in Table 2.
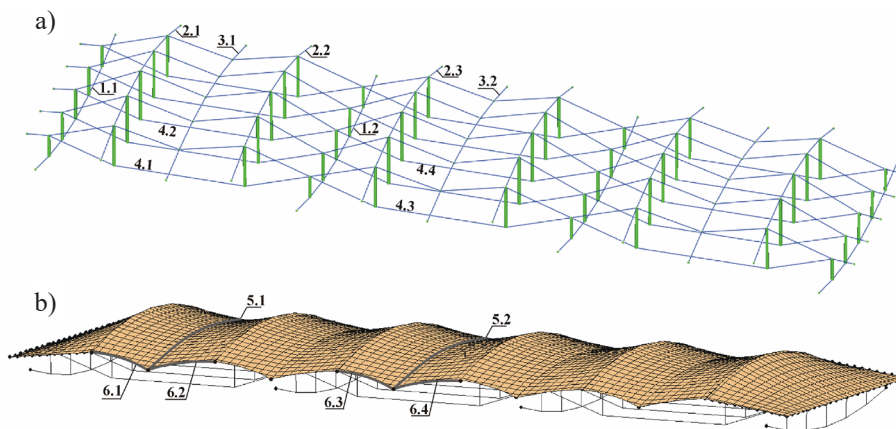

Fig. 9. Cable designation: a) the cables of the roof's frame; b) the cables for tensioning the membrane

Table 2. Correlation coefficients (12) between axial forces and creep elongations of structural elements

Type of the cable	Creep slackening					
	membrane	cables 1	cables 2	ties 3	cables 4	cables 5 and 6
cables 1	−0.16	−0.53	−0.13	–	–	–
cables 2	0.19	−0.37	−0.54	–	−0.18	–
ties 3	0.30	−0.30	0.29	−0.53	−0.37	–
cables 4	−0.19	−0.24	−0.17	–	−0.39	–
cables 5	**−0.62**	−0.20	–	–	−0.18	**−0.78**
cables 6	**−0.93**	−0.23	–	–	–	**−0.83**

Correlation coefficients, having absolute values less than 0.1 are skipped and correlation coefficients, having absolute values greater than 0.6 are highlighted in bold
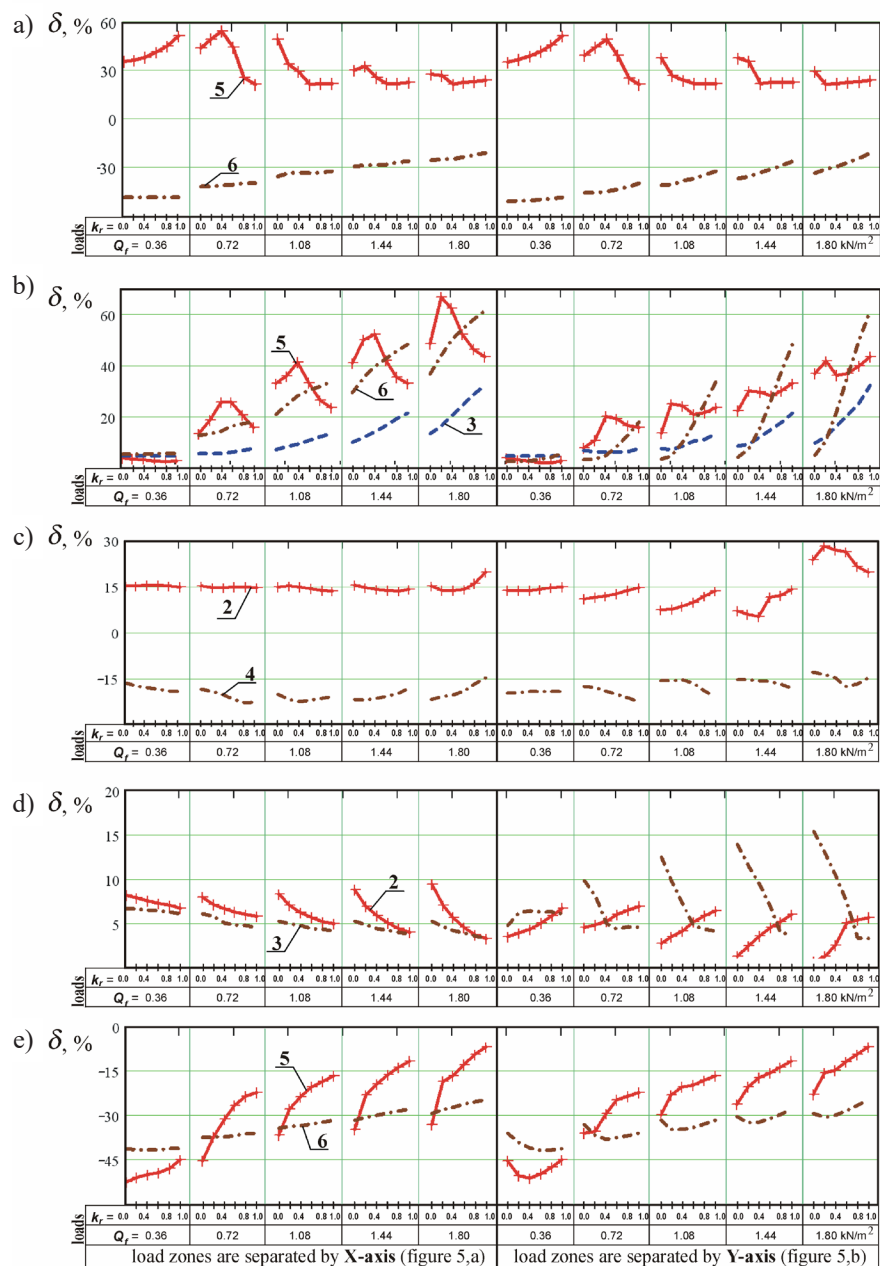
Fig. 10. Graphs of axial force variations δ (9) in the structural elements of the roof under all load cases, given material aging factor: a) membrane tearing along the X-axis (Fig. 3a); b), c) membrane tearing along the Y-axis (Figs. 3b and 3c); d), e) creep slackening of the membrane; 2–6 – types of the cables (Fig. 9)

Most of the correlation coefficients are negative, meaning that axial forces in structural elements tend to diminish in accordance with the growth of creep elongation. The exception is the behavior of ridge cables 2 and ties 3, which are additionally stressed up to 17% (Fig. 10d).

Table 2 also shows a significant correlation between forces in backstay and catenary cables (elements 5 and 6) and creep elongation of the membrane. Slackening of the backstay cables achieves 53%, while for the catenary cables it is confined by 42% (Fig. 10e).

4. Conclusions

The findings presented in this article permit a number of conclusions to be drawn:

– The problem of material aging with respect to the flexible roof structure is considered. Membrane damages and creep elongation are taken into account.

– Backstay and catenary cables are statistically significantly influenced by all the membrane damage

scenarios considered. Axial forces in the backstay cables tend to grow up to 65%. Force variation in the catenary cables depends on the damage type: tearing along the X-axis results in slackening of the catenaries up to 50%, while tearing along the Y-axis brings about stress growth up to 60%.

– Membrane tearing along the Y-axis in the middle of the roof's span significantly influences the ridge cables, longitudinal ties, and transverse bearer cables. The forces in the ridge cables and longitudinal ties increase up to 30%, while axial forces in the transverse bearer cables tend to diminish.

– Creep elongation of the membrane has a significant negative correlation with axial forces in the backstay and catenary cables, while a positive correlation takes place with the ridge cables and the ties.

– The present work contributes to the safety enhancement of cable-membrane structures and the expansion of their scope on permanent building constructions. The results may be used in the life expectancy assessment of flexible roof structures.

References

Asadi, H., Uhlemann, J., Stegmaier, T., Von Arnim, V., & Stranghöner, N. (2017). Investigations into the long-term behavior of fabrics. In K. Bletzinger, E. Oñate, & B. Kröplin (Eds.). *VIII International Conference on Textile Composites and Inflatable Structures*. *Structural membranes 2017. 9–11 october 2017, Munich, Germany* (pp. 217–228), International Center for Numerical Methods in Engineering (CIMNE). http://congress.cimne.com/membranes2017/frontal/Doc/Ebook2017.pdf.

Bridgens, B.N., Gosling, P.D., & Birchall, M.J.S. (2004). Tensile fabric structures: concepts, practice and developments. *The Structural Engineer*, *82*(14), 21–27. https://www.istructe.org/journal/volumes/volume-82-(published-in-2004)/issue-14/tensile-fabric-structures-concepts,-practice-and-d/.

Chesnokov, A.V., & Mikhailov, V.V. (2017a). Cable roof structure with flexible fabric covering. In K. Bletzinger, E. Oñate, & B. Kröplin (Eds.). *VIII International Conference on Textile Composites and Inflatable Structures*. *Structural membranes 2017. 9–11 october 2017, Munich, Germany* (pp. 436–447), International Center for Numerical Methods in Engineering (CIMNE). http://congress.cimne.com/membranes2017/frontal/Doc/Ebook2017.pdf.

Chesnokov, A.V., & Mikhaylov, V.V. (2017b). *Vantovaya konstruktsiya pokrytiya* [Чесноков, А.В., & Михайлов, В.В. (2017b). Вантовая конструкция покрытия]. *Utility model patent* RU169612. https://www.fips.ru/registers-doc-view/fips_servlet?DB=RUPM&DocNumber=169612&TypeFile=html.

Chesnokov, A.V., Mikhaylov, V.V., & Dolmatov, I.V. (2018). Chislennyy algoritm opredeleniya zhestkostnykh parametrov i velichiny predvaritel'nogo napryazheniya vantovoy konstruktsii pokrytiya. *Vestnik Volgogradskogo Gosudarstvennogoarkhiturno-Stroitel'nogo Universiteta*, 52(71), 61–70 [Чесноков, А.В., Михайлов, В.В., & Долматов, И.В. (2018). Численный алгоритм определения жесткостных параметров и величины предварительного напряжения вантовой конструкции покрытия. *Вестник Волгоградского Государственного Архитектурно-Строительного Университета*, *52*(71), 61–70]. https://vgasu.ru/upload/files/science/vestnik_52(71).pdf.

ETA-11/0160 (2018). *European Technical Assessment. PFEIFER Wire Ropes*. Annex C3. https://www.pfeifer.info/out/assets/PFEIFER_WIRE-ROPES_TECHNICAL-APPROVAL-ETA-11-0160_EN.PDF.

Fiúza, A.P.L. (2016). *Polymeric membranes in architecture. Principles and applications in temporary and permanent structures*. Master thesis. Técnico Lisboa.

Forster, B., & Mollaert, M. (2004). *European Design Guide for Tensile Surface Structures*. TensiNet.

Gosling, P.D., Bridgens, B.N., & Zhang, L. (2012). Adoption of a reliability approach for membrane structure analysis. *Structural Safety*, *40*, 39–50. https://doi.org/10.1016/j.strusafe.2012.09.002.

Kupriyanov, V.N. (1986). *Dolgovechnost' tentovykh materialov: Nauchnyye printsipy i metodologii uskorennoy otsenki sroka sluzhby materialov v zadannykh usloviyakh ekspluatatsii*. Dissertatsiya na soiskaniye uchënoy stepeni doktora tekhnicheskikh nauk. Kazanskiy Gosudarstvennyy Arkhitekturno-Stroitel'nyy Universitet, Kazan', Rossiyskaya Federatsiya [Куприянов, В.Н. (1986). *Долговечность тентовых материалов: Научные принципы и методологии ускоренной оценки срока службы материалов в заданных условиях эксплуатации*. Диссертация на соискание учёной степени доктора технических наук. Казанский Государственный Архитектурно-Строительный Университет, Казань, Российская Федерация].

Monjo-Carrio, J. (2015). Understanding and overcoming failures associated with architectural fabric structures. In J.I. Llorens (Eds.). *Fabric Structures in Architecture* (pp. 241–256). Woodhead Publishing.

Mukhamedova, I.Z. (2005). *Issledovaniye protsessov deformirovaniya i destruktsii armirovannykh polimerov*. Dissertatsiya na soiskaniye uchënoy stepeni kandidata fiziko-matematicheskikh nauk. Kazanskiy Gosudarstvennyy Arkhitekturno-Atroitel'nyy Universitet, Kazan', Rossiyskaya Federatsiya [Мухамедова, И.З. (2005). *Исследование процессов деформирования и деструкции армированных полимеров*. Диссертация на соискание учёной степени кандидата физико-математических наук. Казанский Государственный Архитектурно-Строительный Университет, Казань, Российская Федерация].

Rice, J.A. (2007). *Mathematical Statistics and Data Analysis*, 3rd ed., Thomson Learning.

Serge Ferrari Group (2021). *Flexlight Advanced 1502 S2*. https://www.sergeferrari.com/products/flexlight-range/flexlight-advanced-1502-s2.

Ströbel, D., Singer, P., & Holl, J. (2016). Analytical formfinding. *International Journal of Space Structures*, *31*(1), 52–61.

Suleymanov, A.M. (2006). *Eksperimental'no-teoreticheskiye osnovy prognozirovaniya i povysheniya dolgovechnosti materialov myagkikh obolochek stroitel'nogo naznacheniya*. Dissertatsiya na soiskaniye uchënoy stepeni doktora tekhnicheskikh nauk. Kazanskiy Gosudarstvennyy Arkhitekturno-Atroitel'nyy Universitet, Kazan', Rossiyskaya Federatsiya [Сулейманов, А.М. (2006). *Экспериментально-теоретические основы прогнозирования и повышения долговечности материалов мягких оболочек строительного назначения*. Диссертация на соискание учёной степени доктора технических наук. Казанский Государственный Архитектурно-Строительный Университет, Казань, Российская Федерация].

Technet GmbH (2019). *Easy. Lightweight structure design*. https://www.technet-gmbh.com/fileadmin/user_upload/technet/Produktinformationen/Easy/Easy_ProductBrochure.pdf.

Tibert, G. (1999). *Numerical analyses of cable roof structures*. Licentiate Thesis. Royal Institute of Technology, Stockholm, Sweden. https://wiac.info/docgeneratev2?fileurl=https://dlscrib.com/downloadFile/59133df9dc0d60c824959f05&title=%5BPDF%5D+TibertLicThesis&utm_source=dlconvert&utm_medium=queue&utm_campaign=5a00b757e2b6f5ff768c494a.

Wang, C., Abdul-Rahman, H., Wood, L.C., Mohd-Rahim, F.A., Zainon, N., & Saputri, E. (2015). Defects of tensioned membrane structures (TMS) in the Tropics. *Journal of Performance of Constructed Facilities*, *29*(2). https://ascelibrary.org/doi/10.1061/%28ASCE%29CF.1943-5509.0000530.